Int. J. Fuzzy Syst. (2022) 24(8):3781–3795
https://doi.org/10.1007/s40815-022-01368-y

Adaptive Fuzzy Finite-Time Consensus Tracking for High-Order Stochastic Multi-agent Systems with Input Saturation

Xinyu Song[1] · **Lin Zhao**[1]

Received: 26 September 2021 / Revised: 10 February 2022 / Accepted: 4 July 2022 / Published online: 26 August 2022

Abstract In this paper, the finite-time leader-following consensus control for high-order stochastic nonlinear multi-agent systems with input constraints is considered. A finite-time consensus tracking controller based on adaptive fuzzy command filtered backstepping is designed under directed communication topology, and the finite-time command filter is induced to eliminate the computational explosion problem in traditional backstepping. At the same time, a fractional power form-based error compensation method is developed to eliminate filtering error. In addition, the fuzzy logic system is used to approximate the unknown nonlinear functions. It can be shown that the practical finite-time stability in mean square can be assured under the given control method. The simulation results show that the proposed controller is effective and feasible.

Keywords Command filtered backstepping · Finite-time convergence · Stochastic multi-agent systems · Input saturation

1 Introduction

Multi-agent systems (MASs) research is receiving increasing attention in the field of control because to its broad application potential in robot manipulator network, sensor network, and formation control in [1–4]. On the other hand, many real systems technically contain stochastic disturbances, such as the robotic arm operating in a random vibration environment [5, 6] and the spacecraft operating in complex space environment [7, 8]. If these stochastic disturbances are ignored, the designed control algorithms according to deterministic systems will not satisfy the design requirements, so it is time to consider stochastic MASs. In addition, the higher-order nonlinear is a common feature of many MASs, and it is necessary to focus the research on higher-order stochastic nonlinear MASs (SNMASs) [9–13].

Many effective approaches have been proposed for the consensus control of SNMASs, such as the H_∞ control [14, 15], sliding mode control [16], and backstepping control [9]. As one of the most commonly used nonlinear control methods, the backstepping approach is frequently utilized in the consensus control of nonlinear MASs [17–19]. However, the controller contains repeated differentiation of virtual control signals, which may lead to the problem of "complexity explosion" (POCE) when dealing with high-order systems. For this reason, a dynamic surface control is proposed, in which a first-order filter is placed after each virtual control signal and the output signal of the filter is used to replace the differential calculation. Subsequently, the dynamic surface backstepping method is applied to MASs in [10, 20]. However, there is still a flaw in this control algorithm that is how to compensate the filter error, which will make the desired convergence region of tracking error cannot be arrived. Therefore, the command filtered backstepping (CFB) [21, 22] was further developed to introduce a command filter and the error compensation system at each step of the backstepping is used to eliminate filtering error. This method was subsequently extended to multi-agent consensus control [23–27], but most of them do not consider the presence of stochastic disturbances.

✉ Lin Zhao
zhaolin1585@163.com

Xinyu Song
xysong7664@163.com

[1] School of Automation, Qingdao University, Qingdao 266071, People's Republic of China

Actually, the traditional backstepping has been extended to stochastic nonlinear systems [28–30], and the CFB-based controllers has been designed to solve the stochastic nonlinear systems [31–35]. Shahvali and Askari [35] paid attention to the SNMASs and solved the consensus tracking problem by using CFB. However, the control algorithms proposed in the above papers can only guarantee the asymptotic convergence, while the finite-time convergent controller design algorithm has better steady-state performance and anti-disturbance properties [36–45].

To achieve finite-time convergence of higher-order stochastic nonlinear systems, the addition of a power integrator (AAPI) technique [38–40] and finite-time control-based adaptive backstepping [41–45] have been suggested. But the AAPI technique will suffer from a high-gain problem as each step of the stability analysis in backstepping relies on an inequality technique. At the same time, since the virtual control functions of the traditional finite-time backstepping contain fractional power functions, and the controller involves differentiation of the virtual control function, which can lead to the singularity problem [41–45]. As a result, it is time to offer a finite-time convergent controller design algorithm based on CFB for SNMASs. Although the control algorithm was improved in [46] and a finite-time command filtered backstepping (FTCFB) was used to achieve finite-time convergence for high-order stochastic nonlinear systems, the virtual control signals and the error compensation system still use the sign function to guarantee finite-time convergence, which may lead to chattering problem. In addition, [46] only considers the single system and the input saturation constraints are not considered. Actually, each agent often has input saturation constraints in some practical applications, which can lead to serious performance degradation or even system instability if not handled properly. Hence, it is necessary to design an anti-saturation finite-time consensus controller. Furthermore, since the fuzzy logic system (FLS) has strong approximation ability to uncertain nonlinear dynamics and is convenient to combine with backstepping, the adaptive fuzzy backstepping control strategy is used to deal with uncertain dynamics in [9, 26, 38], and is also utilize to solve the control problem of stochastic nonlinear systems with full state constraints and prescribedperformance respectively in [44, 45].

So we will investigate the finite-time consensus tracking for uncertain high-order SNMASs with input saturation using a CFB control approach based on FLS. The main contributions of this paper are as follows:

(1) In contrast to the traditional asymptotically convergent algorithm of consensus tracking for MASs [23–26], we propose the algorithm with finite-time convergence, which can obtain higher tracking accuracy and faster convergence rate.
(2) Compared with the AAPI method [38–40] and traditional finite-time backstepping [41–45], this paper designs a new control law based on FTCFB to avoid the high-gain problem and singularity problem.
(3) Compared to the FTCFB for stochastic systems in [46], we further consider the input saturation, and the design process replaces the sign function with a fraction power function to eliminate chattering of the error compensation siginals.

2 Preliminaries and System Descriptions

2.1 Graph Theory

Consider the case of a MAS with one leader and N followers. The agent is considered as a node, and the topology of the communication network between agents is defined by a directed graph $\mathcal{G} = (\mathcal{V}, \boldsymbol{\varepsilon}, \mathcal{P})$. The directed graph $\mathcal{G}$ is made up of N nodes in a nonempty finite set $\mathcal{V} = \{v_1 ..., v_N\}$, a set of directed edges $\boldsymbol{\varepsilon} \subseteq \mathcal{V} \times \mathcal{V}$, and a weighted adjacency matrix $\mathcal{P} = [\rho_{ij}] \in \mathbf{R}^{N\times N}$. $(v_i, v_j) \in \boldsymbol{\varepsilon}$ is the edge of the directed graph $\mathcal{G}$, indicating that agent j may obtain information from agent i. The element ρ_{ij} in the weighted adjacency matrix $\mathcal{P}$ represents the weight of edge v_{ij}, and ρ_{ij} is non-negative real numbers. If $(v_j, v_i) \in \boldsymbol{\varepsilon}$, then $\rho_{ij} > 0$; otherwise $\rho_{ij} = 0$. Define the set of neighbors for node v_i as $\mathcal{N}_i = \{v_j : (v_j, v_i) \in \boldsymbol{\varepsilon}\}$. A diagonal matrix $\mathcal{D} = diag\{d_i\}$ is defined as the entry matrix of a directed graph, where the diagonal element $d_i = \sum_{j=1}^{N} \rho_{ij}$. $\mathcal{L} = \mathcal{D} - \mathcal{P}$ represents the graph's Laplacian matrix, where

$$l_{ij} = \begin{cases} -\rho_{ij}, i \neq j, \\ \sum\limits_{i=1}^{N} \rho_{ij}, i = j. \end{cases}$$

If there is a directed path from node v_i to node v_j, such as $\{(v_i, v_k), (v_k, v_i), \cdots, (v_m, v_n), (v_n v_j)\}$, then node v_j is reachable from node v_i. If and only if there is a root node generated by at least one leader that can reach all the other nodes, a directed graph contains a spanning tree.

Consider the extension graph $\overline{\mathcal{G}} = (\overline{\mathcal{V}}, \overline{\boldsymbol{\varepsilon}})$, which corresponds to a system with N follower agents and a leader agent 0. $\mathcal{O} = \text{diag}\{o_1, \ldots, o_N\}$ is the leader adjacency matrix, where o_i is a strictly positive constant if an edge exists between nodes 0 and i else $o_i = 0$.

Assumption 1 The root node is the leader node in $\overline{\mathcal{G}}$, which includes a spanning tree.

2.2 Preliminaries and Some Lemmas

The dynamic description of the stochastic system in continuous time is as follows

$$\mathrm{d}\zeta(\mathrm{t}) = \mathrm{F}(\zeta(\mathrm{t}))\mathrm{dt} + \Phi(\zeta(\mathrm{t}))\mathrm{dw}(\mathrm{t}), \zeta(\mathrm{t}_0) = \zeta_0, \tag{1}$$

where $\zeta(t)$ is n-dimensional stochastic state variable, ζ_0 is the stochastic initial condition; $F(\cdot)$ and $g(\cdot)$ are continuous function in $\zeta(t)$, and $w(t)$ is a set of white Gaussian noise process, which is independent of $\zeta(t)$.

Definition 1 [41] The equilibrium of system (1) $\zeta(t) = 0$ is practically finite-time stable in mean square, if there is a stochastic settling time $T(\epsilon, \zeta_0) < \infty$ and ϵ is a positive constant, for $\forall t > t_0 + T$, the system will find $E[\|\zeta(t)\|^2] < \epsilon$.

Definition 2 [41] Define a differential operator as L for $V(\zeta) \in C^2$, which is related to stochastic system (1)

$$LV(\zeta) = \frac{\partial V}{\partial \zeta} F(\zeta(t)) + \frac{1}{2}\mathrm{Tr}\left\{\Phi(\zeta(t))\frac{\partial^2 V}{\partial \zeta^2}\Phi(\zeta(t))\right\}, \tag{2}$$

where Tr represents a matrix trace.

Lemma 1 [27] *When Assumption 1 is met, the eigenvalues of $H = \mathcal{L} + \mathcal{B}$ have positive real parts.*

Lemma 2 [27] *For a continuous function $f(Z)$ delimited on a compact set, there exists a FLS $V^T S(Z)$ such that*

$$\sup_{Z\in\Omega}\left|f(Z) - V^T S(Z)\right| \le \varepsilon, \tag{3}$$

where $\varepsilon > 0$ is a scalar, $V = [V_1, ..., V_M]^T$ is the ideal weight vector, and $S(Z) = [S_1(Z), ..., S_M(Z)]^T / \sum_{i=1}^{M} S_i(Z)$ is the basis function vector and $M > 0$ is the number of FLS nodes. $S_i(Z) = \exp[\frac{-(Z-\gamma_i)^T(Z-\gamma_i)}{w_i^2}], i = 1, 2, ..., M$, where w_i is the width, $\gamma_i = [\gamma_{i1}, ..., \gamma_{in}]^T$ is the center vector.

Lemma 3 [21] *For $z_i \in \mathbf{R}, i = 1, \cdots, K, 0 < \kappa \le 1$, there holds*

$$\left(\sum_{i=1}^{K}|z_i|\right)^{\kappa} \le \sum_{i=1}^{K}|z_i|^{\kappa} \le K^{1-\kappa}\left(\sum_{i=1}^{K}|z_i|\right)^{\kappa}. \tag{4}$$

Lemma 4 [41] *For $x, z \in \mathbf{R}$, $p > 0, q > 0$ and $\alpha(x, z) > 0$,*

$$|x|^p|z|^q \le \frac{p\alpha(x,z)|x|^{p+q}}{p+q} + \frac{q\alpha(x,z)^{-\frac{p}{q}}|z|^{p+q}}{p+q}. \tag{5}$$

Lemma 5 [41] *If there are three positive constants $\Delta, \Gamma, \kappa \in (0, 1)$ and two κ_∞–functions β_1 and β_2 ,which make a C^2 function $W(\zeta(t))$ such that*

$$\begin{cases} \beta_1(\|\zeta(t)\|) \le V(\zeta(t)) \le \beta_2(\|\zeta(t)\|), 0 \le s \le t, \\ W(\zeta(t)) - W(\zeta(s)) \le -\Delta\int_s^t W^{\kappa}(\zeta(v))dv + \Gamma(t-s) \end{cases}.$$

Then, for $\forall t \ge T$, there holds $\|\zeta(t)\| < \epsilon$; where

$$T = \frac{1}{(1-\kappa)\sigma\Delta}\left[V^{1-\kappa}(\zeta(0)) - \left(\frac{\Gamma}{(1-\sigma)\Delta}\right)^{(1-\kappa)/\kappa}\right],$$

$$\epsilon = \beta_1^{-1}\left[([\Gamma/((1-\sigma)\Delta)])^{1/\kappa}\right], 0 < \sigma < 1.$$

2.3 System Descriptions

Based on the description for (1), the SNMASs under the extension graph $\overline{\mathcal{G}}$ in strict-feedback form is described as follows, where each agent is a n-order nonlinear system.

$$\begin{cases} dz_{k,i} = (z_{k,i+1} + f_{k,i}(\bar{z}_{k,i}))\mathrm{d}t + g_{k,i}(\bar{z}_{k,i})\mathrm{d}w, \\ dz_{k,n} = (u_k + f_{k,n}(z_k))\mathrm{d}t + g_{k,n}(z_k)\mathrm{d}w, \\ y_k = z_{k,1}(k \in \mathcal{V}, i = 1, 2, \ldots, n-1), \end{cases} \tag{6}$$

where $z_k = \left[z_{k,1}, z_{k,2}, \cdots, z_{k,n}\right]^T \in \mathbf{R}^n$ is the state vector with $\bar{z}_{k,i} = \left[z_{k,1}, z_{k,2}, \cdots, z_{k,i}\right]^T \in \mathbf{R}^i$, $u_k, y_k \in \mathbf{R}$ are the input and output of the agents. $f_{k,i}(\cdot) : \mathbf{R}^i \to \mathbf{R}$ and $g_{k,i}(\cdot) : \mathbf{R}^i \to \mathbf{R}^r$ are assumed to be the unknown and smooth nonlinear functions; w represents an r-dimensional Brownian motion. $y_d \in \mathbf{R}$ is denoted as the output of the leader.

Assumption 2 Assume that y_d and its first-order derivative $\dot{y_d}$ are smooth, bounded, and known functions and denote $y_d \in \mathbf{R}$.

Remark 1 Assumption 2 is a general assumption for CFB design as in [21–26]. Note that $\dot{y}_d^{(i)}, i = 1, \cdots, n$ must be used in the design for traditional backstepping, but the CFB only uses y_d and $\dot{y}_d$, which is less stringent for the desired signal.

Assumption 3 Let $\Omega_d \subset \mathbf{R}^n$ be an open set that contains the origin, $z_k(0)$ and y_d. $z_k(0)$, the functions $f_{k,i}(\cdot), f_{k,i}^{(p)}(\cdot)$ and $g_{k,i}^{(p)}(\cdot)$ are bounded on $\bar{\Omega}_d$ for $p = 1, \cdots, (n-s)$.

The input $u_k \in \mathbf{R}$ is saturated nonlinearly represented by

$$u_k = \mathrm{sat}(\tau_k) = \begin{cases} u_{k,\max}, & \tau_k \ge u_{k,\max} \\ \tau_k, & u_{k,\min} < \tau_k < u_{k,\max}, \\ u_{k,\min}, & \tau_k \le u_{k,\min} \end{cases}$$

and $u_{k,\max} > 0, u_{k,\min} < 0$ are the upper and lower known limits of input. Define

$$\eta(\tau_k)=\begin{cases} u_{k,\max}\times\tanh\left(\dfrac{\tau_k}{u_{k,\max}}\right), & \tau_k\geq 0,\\ u_{k,\min}\times\tanh\left(\dfrac{\tau_k}{u_{k,\min}}\right), & \tau_k<0, \end{cases}$$

and $|\tilde{\eta}(\tau_k)|=|\mathrm{sat}(\tau_k)-\eta(\tau_k)|\leq \max\{u_{k,\max}(1-\tanh(1)),u_{k,\min}(1-\tanh(1))\}\triangleq\bar{\eta}_k$, then $u_k=\mathrm{sat}(\tau_k)=\eta(\tau_k)+\tilde{\eta}(\tau_k)$.

3 Main Results

In this section, a new adaptive FTCFB control strategy is designed to ensure that the output y_k can track a given trajectory y_d in finite-time, where the FLS $V_{k,i}^T S_{k,i}$ will be utilized to approximate an unknown function $\bar{f}_{k,i}$ in each step of the FTCFB procedure. We define a constant $\theta_{k,i}=\|V_{k,i}\|^2,(i=1,\ldots,n)$, $\hat{\theta}_{k,i}$ as the estimate of $\theta_{k,i}$ and $\tilde{\theta}_{k,i}=\theta_{k,i}-\hat{\theta}_{k,i}$ as an estimate error. The block diagram of the proposed adaptive FTCFB control system with FLS can be found in Fig. 1.

3.1 Controller Design

Define the consensus tracking errors $\mu_{k,i}$ as

$$\begin{cases} \mu_{k,1}=\sum_{j=1}^{N}\rho_{k,j}(y_k-y_j)+o_k(y_k-y_d),\\ \mu_{k,i}=z_{k,i}-\varphi_{k,i}(i=2,\ldots,n). \end{cases} \tag{7}$$

in which $\varphi_{k,i}$ is the output of FTCF and the virtual signal $\chi_{k,i-1}$ is the input. For $k\in\mathcal{V}$, $i=1,\cdots,n-1$, the FTCF is designed as

$$\begin{aligned} \dot{\Psi}_{k,i,1}=&\Pi_{k,i,1},\\ \Pi_{k,i,1}=&-\varsigma_{k,i,1}\left|\Psi_{k,i,1}-\chi_{k,i-1}\right|^{\frac{1}{2}}\mathrm{sign}(\Psi_{\mathrm{k,i,1}}\\ &-\chi_{k,i-1})+\Psi_{k,i,2},\\ \dot{\Psi}_{k,i,2}=&-\varsigma_{k,i,2}\mathrm{sign}\left(\Psi_{\mathrm{k,i,2}}-\Pi_{\mathrm{k,i,1}}.\right) \end{aligned} \tag{8}$$

with $\varphi_{k,i}(t)=\Psi_{k,i,1}(t)$ and $\dot{\varphi}_{k,i}(t)=\Pi_{k,i,1}(t)$, and $\varsigma_{k,i,1}>0$ and $\varsigma_{k,i,2}>0$ are filter gains.

Lemma 6 [47] *For the case of absent input noise, that is $\chi_{k,i-1}=\chi_{k,i-1,0}$, if choosing $\varsigma_{k,i,1}$ and $\varsigma_{k,i,2}$ properly, the following equations are achieved in finite-time*

$$\Psi_{k,i,1}=\chi_{k,i-1,0},\Pi_{k,i,1}=\dot{\chi}_{k,i-1,0}. \tag{9}$$

For the case of present input noise, assume the input noise satisfies $|\chi_{k,i-1}-\chi_{i-1,0}|\leq\Xi_{k,i-1}$, where $\Xi_{k,i-1}$ is a positive constant. Then the following inequality holds in finite-time

$$\begin{aligned} &\left|\Psi_{k,i,1}-\chi_{k,i-1,0}\right|\leq\Theta_{k,i-1}\Xi_{k,i}=\pi_{k,i-1,1},\\ &\left|\Pi_{k,i,1}-\dot{\chi}_{k,i-1,0}\right|\leq\Upsilon_{k,i-1}\Xi_{k,i-1}^{\frac{1}{2}}=\pi_{k,i-1,2}. \end{aligned} \tag{10}$$

where $\Theta_{k,i-1}>0$ and $\Upsilon_{k,i-1}>0$ are constants.

Remark 2 Taking the virtual controller $\chi_{k,i-1}$ as input, the $\varphi_{k,i}$ and its first-order derivative $\dot{\varphi}_{k,i}$ can be obtained. Moreover, the command filter in this paper can not only guarantee the filter effect of $\chi_{k,i-1}$, but also achieve stability in a finite-time compared with [23–26, 31–34].

The controller τ_k and virtual control signals $\chi_{k,i}(i=1,\cdots,n-1)$ are designed as follows

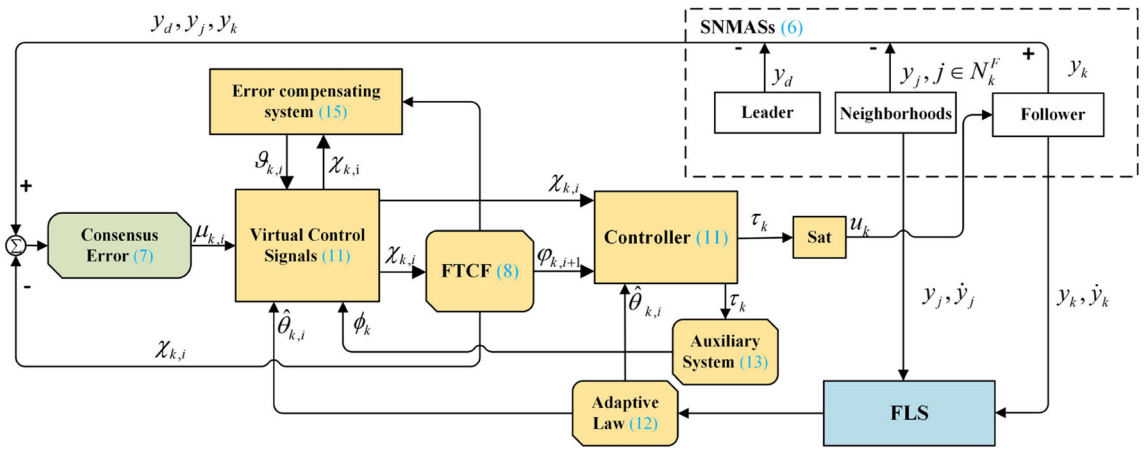

Fig. 1 Block diagram of adaptive FTCFB algorithm

$$\begin{aligned}
\chi_{k,1} =& \frac{1}{\rho_k}\Bigg(- s_{k,1} v_{k,1}^{\kappa} - \frac{3}{4}\Big(1 + t_{k,1}\Big) v_{k,1} + \sum_{j=1}^{N} \rho_{k,j} z_{j,2} \\
& - \frac{1}{2b_{k,1}^2} \hat{\theta}_{k,1} v_{k,1}{}^3 S_{k,1}^T S_{k,1} + o_k \dot{y_d}) - \frac{3}{4} v_{k,1}, \\
\chi_{k,2} =& -s_{k,2} v_{k,2}^{\kappa} - \frac{3}{4}(2 + t_{k,2}) v_{k,2} \\
& - \frac{1}{2b_{k,2}^2} \hat{\theta}_{k,2} v_{k,2}{}^3 S_{k,2}^T S_{k,2} - \frac{1}{4} \rho_k v_{k,1}, \\
\chi_{k,i} =& -s_{k,i} v_{k,i}^{\kappa} - \left(\frac{7}{4} + \frac{3}{4} t_{k,i}\right) v_{k,i} \\
& - \frac{1}{2b_{k,i}^2} \hat{\theta}_{k,i} v_{k,i}{}^3 S_{k,i}^T S_{k,i}, (i = 3, \ldots, n-2), \\
\chi_{k,n-1} =& -s_{k,n-1} v_{k,n-1}^{\kappa} - (\frac{7}{4} + \frac{3}{4} t_{k,n-1}) v_{k,n-1} \\
& - \frac{1}{2b_{k,n-1}^2} \hat{\theta}_{k,n-1} v_{k,n-1}{}^3 S_{k,n-1}^T S_{k,n-1} - \phi_k, \\
\chi_{k,n} =& -s_{k,n} v_{k,n}^{\kappa} - (1 + \frac{3}{4} t_{k,n}) v_{k,n} \\
& - \frac{1}{2b_{k,n}^2} \hat{\theta}_{k,n} v_{k,n-1}{}^3 S_{k,n}^T S_{k,n},
\end{aligned} \tag{11}$$

where $\rho_k = o_k + \sum_{j=1}^{N} \rho_{k,j}, 0 < \kappa < 1$,$s_{k,i} > 0, t_{k,i} > 0$ $(i = 1, \ldots, n)$ are designed constants. The updating process of $\hat{\theta}_{k,i}$ is designed as

$$\dot{\hat{\theta}}_{k,i} = -r_{k,i} \hat{\theta}_{k,i} + \frac{\lambda_{k,i}}{2b_{k,i}^2} v_{k,i}^6 S_{k,i}^T S_{k,i}, \tag{12}$$

where $r_{k,i} > 0$ is a constant.

ϕ_k is an auxiliary system defined as follows

$$\dot{\phi}_k = -\phi_k + \eta(\tau_k) - \tau_k. \tag{13}$$

$v_{k,i}$ is the compensated tracking error defined by

$$\begin{cases} v_{k,\mathrm{i}} = \mu_{k,\mathrm{i}} - \vartheta_{k,\mathrm{i}} (i = 1, \ldots, n-1), \\ v_{k,n} = \mu_{k,n} - \vartheta_{k,n} - \phi_k. \end{cases} \tag{14}$$

$\vartheta_{k,i}$ is the error compensation system defined by

$$\begin{aligned}
\dot{\vartheta}_{k,1} =& - t_{k,1} \vartheta_{k,1} - s_{k,1} \vartheta_{k,1}^{\kappa} \\
& - \rho_k[(\varphi_{k,2} - \chi_{k,1}) + \vartheta_{k,2}], \\
\dot{\vartheta}_{k,\mathrm{i}} =& - t_{k,i} \vartheta_{k,\mathrm{i}} - s_{k,i} \vartheta_{k,i}^{\kappa} - (\varphi_{k,i+1} \\
& - \chi_{k,i}) + \vartheta_{k,\mathrm{i}+1} (i = 2, \ldots, n), \\
\dot{\vartheta}_{k,n} =& - t_{k,n} \vartheta_{k,n} - s_{k,n} \vartheta_{k,n}^{\kappa},
\end{aligned} \tag{15}$$

with $\vartheta_{k,i}(0) = 0 (i = 1, \cdots, n)$, and $t_{k,i} > 0$, $s_{k,i} > 0$ are designed constants.

Remark 3 In the traditional finite-time backstepping-based controllers design for nonlinear systems in [41–45], since the fraction power is used, the singularity problem may exist since the derivative of virtual control function should be used. In the proposed algorithm, the command filter serves to approximate the differentiation of the virtual control signal, thus can avoid the singularity problem.

Remark 4 In order to overcome the influence of input saturation on control performance, an auxiliary system (13) is introduced in the controller design, which can guarantee the actual control input τ_k can be designed.

Remark 5 In order to realize the finite-time control of the closed-loop system, the fraction power function is designed in the virtual control signal $\chi_{k,i}$ and the error compensation system $\vartheta_{k,i}$. Compared with the signal function selected by [46], the controller in this paper is more smooth.

Now, we perform the recursive control design in the following steps.

Step 1 Considering the stochastic system (6), from $v_{k,1} = \mu_{k,1} - \vartheta_{k,1}$, we have

$$\begin{aligned}
dv_{k,1} =& [\rho_k(z_{k,2} + f_{k,1}) - \sum_{j=1}^{N} \rho_{k,j}(z_{j,2} + f_{j,1}) \\
& - o_k \dot{y_d} - \dot{\vartheta}_{k,1}]\mathrm{dt} + \mathrm{G}_{\mathrm{k},1}^{\mathrm{T}} \mathrm{dw},
\end{aligned} \tag{16}$$

where $G_{k,1} = \rho_k g_{k,1} - \sum_{j=1}^{N} \rho_{k,j} g_{k,1}$.

Choose the Lyapunov function as follows

$$W_{k,1} = \frac{1}{4} v_{\mathrm{k},1}^4 + \frac{\theta_{\mathrm{k},1}^2}{2\lambda_{\mathrm{k},1}}, \tag{17}$$

where $\tilde{\theta}_{k,1} = \theta_{k,1} - \hat{\theta}_{k,1}$, and $\lambda_{k,1} > 0$ is a constant.

$$\begin{aligned}
LW_{k,1} =& v_{k,1}^3 [\rho_k(\chi_{k,1} + \mu_{k,2} + (\varphi_{k,2} - \chi_{k,1}) \\
& + f_{k,1}) - \sum_{j=1}^{N} \rho_{k,j}(z_{j,2} + f_{j,1}) - o_k \dot{y_d} \\
& - \dot{\vartheta}_{k,1}] + \frac{3}{2} v_{k,1}^2 \left\| G_{k,1} \right\|^2 - \frac{\tilde{\theta}_{k,1} \dot{\hat{\theta}}_{k,1}}{\lambda_{k,1}}.
\end{aligned} \tag{18}$$

Substituting (15) into (18) yields

$$\begin{aligned}
LW_{k,1} \le& v_{k,1}^3 [\rho_k(\chi_{k,1} + v_{k,2} + f_{k,1}) \\
& - o_k \dot{y_d} - \sum_{j=1}^{N} \rho_{k,j}(z_{j,2} + f_{j,1}) \\
& + t_{k,1} \vartheta_{k,1} + s_{k,1} \vartheta_{k,1}^{\kappa}] \\
& + \frac{3}{2} v_{k,1}^2 \left\| G_{k,1} \right\|^2 - \frac{\tilde{\theta}_{k,1} \dot{\hat{\theta}}_{k,1}}{\lambda_{k,1}},
\end{aligned} \tag{19}$$

By applying Young's inequality, we have

$$v_{k,1}^3 v_{k,2} \le \frac{3}{4} v_{k,1}^4 + \frac{1}{4} v_{k,2}^4, \tag{20}$$

$$\frac{3}{2} v_{k,1}^2 \left\| G_{k,1} \right\|^2 \le \frac{3}{4} v_{k,1}^4 l_{k,1}^{-2} \left\| G_{k,1} \right\|^4 + \frac{1}{4} l_{k,1}^2. \tag{21}$$

where $l_{k,1} > 0$. Substituting (20) and (21) into (19) gives

$$\begin{aligned} LW_{k,1} \le & v_{k,1}^3 [\rho_k (\chi_{k,1} + \frac{3}{4} v_{k,1} + f_{k,1}) \\ & - \sum_{j=1}^{N} \rho_{k,j} (z_{j,2} + f_{j,1}) - o_k \dot{y_d} \\ & + t_{k,1} \vartheta_{k,1} + s_{k,1} \vartheta_{k,1}^{\kappa} \\ & + \frac{3}{4} v_{k,1} l_{k,1}^{-2} \left\| G_{k,1} \right\|^2] - \frac{\tilde{\theta}_{k,1} \dot{\hat{\theta}}_{k,1}}{\lambda_{k,1}} \\ & + \frac{1}{4} l_{k,1}^2 + \frac{1}{4} \rho_k v_{k,2}^4. \end{aligned} \tag{22}$$

Let $\bar{f_{k,1}} = \rho_k f_{k,1} - \sum_{j=1}^{N} \rho_{k,j} f_{j,1} + \frac{3}{4} v_{k,1} l_{k,1}^{-2} \left\| G_{k,1} \right\|^2$, we adopt a FLS $V_{k,1}^T S_{k,1}$ to approximate it, that is $\forall \varepsilon_{k,1} > 0$, one has

$$\bar{f_{k,1}} = V_{k,1}^T S_{k,1} + \delta_1, |\delta_{k,1}| \le \varepsilon_{k,1}, \tag{23}$$

By using Young's inequality, we obtain

$$\begin{aligned} v_{k,1}^3 \bar{f}_{k,1} \le & \frac{1}{2b_{k,1}^2} v_{k,1}^6 \theta_{k,1} S_{k,1}^T S_{k,1} \\ & + \frac{b_{k,1}^2}{2} + \frac{3}{4} v_{k,1}^4 + \frac{1}{4} \varepsilon_{k,1}^4, \end{aligned} \tag{24}$$

Similarly, we have

$$t_{k,1} v_{k,1}^3 \vartheta_{k,1} \le \frac{3}{4} t_{k,1} v_{k,1}^4 + \frac{1}{4} t_{k,1} \vartheta_{k,1}^4. \tag{25}$$

Substituting (24) - (25) into (22), one has

$$\begin{aligned} LW_{k,1} \le & v_{k,1}^3 \left[\rho_k (\chi_{k,1} + \frac{3}{2} v_{k,1}) - o_k \dot{y_d} \right. \\ & - \sum_{j=1}^{N} \rho_{k,j} z_{j,2} + \frac{1}{2b_{k,1}^2} v_{k,1}^3 \theta_{k,1} S_{k,1}^T S_{k,1} \\ & \left. + \frac{3}{4} t_{k,1} v_{k,1} + s_{k,1} \vartheta_{k,1}^{\kappa} \right] - \frac{1}{\lambda_{k,1}} \tilde{\theta}_{k,1} \dot{\hat{\theta}}_{k,1} \\ & + \frac{1}{4} t_{k,1} \vartheta_{k,1}^4 + \frac{1}{4} \rho_k v_{k,2}^4 + \Gamma_{k,1}, \end{aligned} \tag{26}$$

where $\Gamma_{k,1} = \frac{1}{4} l_{k,1}^2 + \rho_k (\frac{b_{k,1}^2}{2} + \frac{1}{4} \varepsilon_{k,1}^4)$.

According to the Lemma 4, we have

$$s_{k,1} v_{k,1}^3 \vartheta_{k,1}^{\kappa} \le \frac{3 s_{k,1}}{\kappa + 3} v_{k,1}^{\kappa+3} + \frac{\kappa s_{k,1}}{\kappa + 3} \vartheta_{k,1}^{\kappa+3}, \tag{27}$$

Then, substituting (11) - (12) and (27) into (26), one has

$$\begin{aligned} LW_{k,1} \le & -\frac{\kappa}{\kappa + 3} s_{k,1} v_{k,1}^{\kappa+3} + \frac{\kappa}{\kappa + 3} s_{k,1} \vartheta_{k,1}^{\kappa+3} \\ & + \frac{r_{k,1}}{\lambda_{k,1}} \tilde{\theta}_{k,1} \hat{\theta}_{k,1} + \frac{1}{4} t_{k,1} \vartheta_{k,1}^4 \\ & + \frac{1}{4} \rho_k v_{k,2}^4 + \Gamma_{k,1}. \end{aligned} \tag{28}$$

Step h$(h = 2, \cdots, n-2)$: From $v_{k,\mathrm{h}} = \mu_{k,\mathrm{h}} - \vartheta_{k,\mathrm{h}}$, we have

$$\begin{aligned} dv_{k,h} = & (z_{k,h+1} + f_{k,h} \\ & - L\varphi_{k,h} - \dot{\vartheta}_{k,\mathrm{h}}) \mathrm{dt} + \mathrm{G}_{\mathrm{k,h}}^{\mathrm{T}} \mathrm{dw}, \end{aligned} \tag{29}$$

where $G_{k,h} = g_{k,h} - \sum_{i=1}^{h-1} \frac{\partial \varphi_{k,i}}{\partial z_{k,h}} g_{k,i}$, and $L\varphi_{k,h}$ can be got by using the L-operator on $\varphi_{k,h}$.

Choose the following Lyapunov function

$$W_{k,h} = \mathrm{W}_{\mathrm{k,h-1}} + \frac{1}{4} v_{\mathrm{k,h}}^4 + \frac{\tilde{\theta}_{\mathrm{k,h}}^2}{2\lambda_{\mathrm{k,h}}}, \tag{30}$$

where $\lambda_{k,i} > 0$ is a constant. From the formula (29), we have

$$\begin{aligned} LW_{k,\mathrm{h}} = & LW_{k,h-1} + v_{k,h}^3 (\chi_{k,h} + \mu_{k,h+1} \\ & + (\varphi_{k,h+1} - \chi_{k,h}) + f_{k,h} - L\varphi_{k,h} \\ & - \dot{\vartheta}_{k,h}) + \frac{3}{2} v_{k,h}^2 \left\| G_{k,h} \right\|^2 - \frac{\tilde{\theta}_{k,h} \dot{\hat{\theta}}_{k,h}}{\lambda_{k,h}}. \end{aligned} \tag{31}$$

Similarly to step 1, we obtain

$$\begin{aligned} LW_{k,\mathrm{h}} \le & LW_{k,h-1} + v_{k,h}^3 \Big(\chi_{k,h} \\ & + \frac{3}{4} (1 + t_{k,h}) v_{k,h} + f_{k,h} \\ & - L\varphi_{k,h} + s_{k,h} \vartheta_{k,h}^{\kappa} \\ & + \frac{3}{4} v_{k,h} l_{k,h}^{-2} \left\| G_{k,h} \right\|^4 \Big) \\ & - \frac{1}{\lambda_{k,h}} \tilde{\theta}_{k,h} \dot{\hat{\theta}}_{k,h} + \frac{1}{4} t_{k,h} \vartheta_{k,h}^4 \\ & + \frac{1}{4} l_{k,h}^2 + \frac{1}{4} v_{h+1}^4. \end{aligned} \tag{32}$$

Let $\bar{f_{k,h}} = \mathrm{f_{k,h}} - \mathrm{L}\varphi_{\mathrm{k,h}} + \frac{3}{4} v_{\mathrm{k,h}} \mathrm{l}_{\mathrm{k,h}}^{-2} \left\| \mathrm{G_{k,h}} \right\|^4$, then according to Lemmas 2 and 4 and using Young's inequality, we obtain

$$\begin{aligned} LW_{k,\mathrm{h}} \le & LW_{k,h-1} + v_{k,h}^3(\chi_{k,h} \\ & + \frac{3}{4}(2+t_{k,h})v_{k,h} + s_{k,h}\vartheta_{k,h}^{\kappa} \\ & + \frac{1}{2\mathrm{b}_{\mathrm{k,h}}^2} v_{k,h}^3 \theta_{k,h} S_{k,h}^T S_{k,h}) \\ & - \frac{1}{\lambda_{k,h}} \tilde{\theta}_{k,h}\dot{\hat{\theta}}_{k,h} + \frac{1}{4} t_{k,h}\vartheta_{k,h}^4 \\ & + \Gamma_{k,i} + \frac{1}{4} v_{h+1}^4, \end{aligned} \tag{33}$$

where $\Gamma_{k,h} = \frac{1}{4} l_{k,h}^2 + \frac{b_{k,h}^2}{2} + \frac{1}{4}\varepsilon_{k,h}^4$.

Then, similarly to step 1 , substituting (11–12) into (33), one has

$$\begin{aligned} LW_{k,\mathrm{h}} \le & -\sum_{i=1}^{h} \frac{\kappa}{\kappa+3} s_{k,i} v_{k,i}^{\kappa+3} \\ & + \sum_{i=1}^{h} \frac{\kappa}{\kappa+3} s_{k,i} \vartheta_{k,i}^{\kappa+3} \\ & + \sum_{i=1}^{h} \frac{r_{k,i}}{\lambda_{k,i}} \tilde{\theta}_{k,i}\hat{\theta}_{k,i} \\ & + \sum_{i=1}^{h} \frac{1}{4} t_{k,i}\vartheta_{k,i}^4 + \sum_{i=1}^{h} \Gamma_h + \frac{1}{4} v_{h+1}^4. \end{aligned} \tag{34}$$

Step n-1 Similarly, we have the following stochastic Lyapunov function

$$W_{k,n-1} = \mathrm{W}_{\mathrm{k,n-2}} + \frac{1}{4} v_{\mathrm{k,n-1}}^4 + \frac{\theta_{\mathrm{k,n-1}}^2}{2\lambda_{\mathrm{k,n-1}}}, \tag{35}$$

where $\lambda_{k,n-1} > 0$ is a constant.

Using L-operator on $W_{k,n-1}$, then substituting (15), we have

$$\begin{aligned} LW_{k,n-1} \le & LW_{k,n-2} + v_{k,n-1}^3(\chi_{k,n-1} \\ & + (\mu_{k,n} - \vartheta_{k,n}) \\ & + (\varphi_{k,n} - \chi_{k,n-1}) + f_{k,n-1} \\ & - L\varphi_{k,n-1} + t_{k,h}\vartheta_{k,h} \\ & + s_{k,h}\vartheta_{k,h}^{\kappa}) + \frac{3}{2} v_{k,n-1}^2 \left\| G_{k,n-1} \right\|^2 \\ & - \frac{1}{\lambda_{k,n-1}} \tilde{\theta}_{k,n-1}\dot{\hat{\theta}}_{k,n-1}. \end{aligned} \tag{36}$$

Using Lemma 4 yields

$$\begin{aligned} & s_{k,n-1} v_{k,n-1}^3 \vartheta_{k,n-1}^{\kappa} \\ & \le \frac{3 s_{k,n-1}}{\kappa+3} v_{k,n-1}^{\kappa+3} + \frac{\kappa s_{k,n-1}}{\kappa+3} \vartheta_{k,n-1}^{\kappa+3}. \end{aligned} \tag{37}$$

Similarly to step 1, substituting (11–12) and (37) into (36) yields

$$\begin{aligned} LW_{k,n-1} \le & -\sum_{i=1}^{n-1} \frac{\kappa}{\kappa+3} s_{k,i} v_{k,i}^{\kappa+3} \\ & + \sum_{i=1}^{n-1} \frac{\kappa}{\kappa+3} s_{k,i} \vartheta_{k,i}^{\kappa+3} + \sum_{i=1}^{n-1} \frac{1}{4} t_{k,i}\vartheta_{k,i}^4 \\ & + \sum_{i=1}^{n-1} \frac{r_{k,n-1}}{\lambda_{k,n-1}} \tilde{\theta}_{k,n-1}\dot{\hat{\theta}}_{k,n-1} \\ & + \sum_{i=1}^{n-1} \Gamma_{k,i} + \frac{1}{4} v_{k,n}^4. \end{aligned} \tag{38}$$

Step n According to the Itô formula, $dv_{k,n}$ can be induced as follows:

$$\begin{aligned} dv_{k,n} = & (u_k + f_{k,n} - L\varphi_{k,n} \\ & - \dot{\vartheta}_{k,n} - \dot{\phi}_k)\mathrm{dt} + \mathrm{G}_{\mathrm{k,n}}^{\mathrm{T}}\mathrm{dw}, \end{aligned} \tag{39}$$

where $G_{k,n} = g_{k,n} - \sum_{h=1}^{n-1} \frac{\partial \varphi_{k,n}}{\partial z_{k,h}} g_{k,h}$.

Choose the following stochastic Lyapunov function

$$W_{k,n} = \mathrm{W}_{\mathrm{k,n-1}} + \frac{1}{4} v_{\mathrm{k,n}}^4 + \frac{\theta_{\mathrm{k,n}}^2}{2\lambda_{\mathrm{k,n}}}, \tag{40}$$

where $\lambda_{k,n} > 0$ is a constant. Then, we have

$$\begin{aligned} LW_{k,n} \le & LW_{k,n-1} + v_{k,n}^3(u_k + f_{k,n} \\ & - L\varphi_{k,n} - \dot{\vartheta}_{k,n} - \dot{\phi}_k) \\ & + \frac{3}{2} v_{k,n}^2 \left\| G_{k,n} \right\|^2 - \frac{\tilde{\theta}_{k,n}\dot{\hat{\theta}}_{k,n}}{\lambda_{k,n}}. \end{aligned} \tag{41}$$

Similarly to step 1, substituting $\dot{\vartheta}_{k,n}$, $\dot{\phi}_k$, and applying Young's inequality, we have

$$\begin{aligned} LW_{k,n} \le & LW_{k,n-1} + v_{k,n}^3(\tau_k \\ & + \frac{3}{4}(1+t_{k,n})v_{k,n} + s_{k,n}\vartheta_{k,n}^{\kappa} \\ & + \frac{1}{2\mathrm{b}_{\mathrm{k,n}}^2} v_{k,n}^3 \theta_{k,n} S_{k,n}^T S_{k,n}) \\ & - \frac{1}{\lambda_{k,n}} \tilde{\theta}_{k,n}\dot{\hat{\theta}}_{k,n} + \frac{1}{4} t_{k,n}\vartheta_{k,n}^4 + \Gamma_{k,n}, \end{aligned} \tag{42}$$

where $\Gamma_{k,n} = \frac{1}{4} l_{k,n}^2 + \frac{b_{k,n}^2}{2} + \frac{1}{4}\varepsilon_{k,n}^4 + \frac{1}{4}\bar{\eta}_k^4$. Then, substituting (11) and (12) into (42), one has

$$\begin{aligned} LW_{k,n} \leq & -\sum_{i=1}^{n}\frac{\kappa}{\kappa+3}s_{k,i}v_{k,i}^{\kappa+3} \\ & +\sum_{i=1}^{n}\frac{\kappa}{\kappa+3}s_{k,i}\vartheta_{k,i}^{\kappa+3} \\ & +\sum_{i=1}^{n}\frac{r_{k,i}}{\lambda_{k,i}}\tilde{\theta}_{k,i}\hat{\theta}_{k,i} \\ & +\sum_{i=1}^{n}\frac{1}{4}t_{k,i}\vartheta_{k,i}^{4}+\sum_{i=1}^{n}\Gamma_{k,i}. \end{aligned} \tag{43}$$

3.2 Stability Analysis

Theorem 1 *Consider the SNMASs* (6) *with Assumptions* 1-3, *if FTCF is chosen as in* (8), *the error compensation system is designed as in* (15), *the virtual signals* $\chi_{k,i}, (k \in \mathcal{V}; i = k = 1, \ldots, n-1)$ *and controller* u_k *are constructed as in* (11) *with the adaptive updating law* (12) *and auxiliary system* (13), *then the tracking error* $y_k - y_d (k \in \mathcal{V})$ *is practically finite-time stable in mean square and all signals in the closed-loop system are bounded in mean square in finite-time.*

Proof For the error compensation system, choose the following Lyapunov function

$$\bar{W}_k = \sum_{\mathrm{i}=1}^{\mathrm{n}}\frac{\vartheta_{\mathrm{k,i}}^{4}}{4}. \tag{44}$$

Then, we have

$$\begin{aligned} L\bar{W}_k =& (\vartheta_{k,1}^{3}\dot{\vartheta}_{k,1}+\vartheta_{k,2}^{3}\dot{\vartheta}_{k,2}+\cdots+\vartheta_{k,n_k}^{3}\dot{\vartheta}_{k,n}) \\ =& -\sum_{i=1}^{n}t_{k,i}\vartheta_{k,i}^{4}-\sum_{i=1}^{n}s_{k,i}\vartheta_{i}^{\kappa+3} \\ & +(o_k+\sum_{j=1}^{N}\rho_{k,j})[\vartheta_{k,1}^{3}(\varphi_{k,2}-\chi_{k,1}) \\ & +\vartheta_{k,2}^{3}\vartheta_{k,2}]+\sum_{i=2}^{n-1}\vartheta_{k,i}^{3}\vartheta_{k,\mathrm{i}+1} \\ & +\sum_{i=2}^{n-1}\vartheta_{k,i}^{3}(\varphi_{k,i+1}-\chi_{k,i}). \end{aligned} \tag{45}$$

Based on Lemma 6, the inequality $|\varphi_{k,i+1}-\chi_{k,i,1}| \leq \pi_{k,i}$ will hold at a finite-time T. Applying the Young's inequality, we have

$$\vartheta_{k,i,1}^{3}\pi_{k,i} \leq \frac{3}{4}\vartheta_{k,i}^{4}+\frac{1}{4}\pi_{k,i,1}^{4}, \tag{46}$$

$$\vartheta_{k,i}^{3}\vartheta_{k,\mathrm{i}+1} \leq \frac{3}{4}\vartheta_{k,i}^{4}+\frac{1}{4}\vartheta_{k,i+1}^{4}. \tag{47}$$

Then, we have

$$\begin{aligned} L\bar{W}_k \leq & -(t_{k,1}-\frac{3}{2}(o_k+\sum_{j=1}^{N}\rho_{k,j}))\vartheta_{k,1}^{4} \\ & -(t_{k,2}-\frac{3}{2}-\frac{1}{4}(o_k+\sum_{j=1}^{N}\rho_{k,j}))\vartheta_{k,2}^{4} \\ & -(t_{k,3}-\frac{7}{4})\vartheta_{k,3}^{4}-\cdots-(t_{k,n}-\frac{1}{4})\vartheta_{k,n}^{4} \\ & -\sum_{i=1}^{n}s_{k,i}\vartheta_{i}^{\gamma+3}+\bar{\Gamma}_k. \end{aligned} \tag{48}$$

where $\bar{\Gamma}_k = \frac{1}{4}(o_k+\sum_{j=1}^{N}\rho_{k,j})\pi_{k,i,1}^{4}+\sum_{i=2}^{n-1}\frac{\pi_{k,i,1}^{4}}{4}$. Moreover, we get

$$\frac{r_{k,i}}{\lambda_{k,i}}\tilde{\theta}_{k,i}\hat{\theta}_{k,i} \leq -\frac{r_{k,i}}{2\lambda_{k,i}}\tilde{\theta}_{k,i}^{2}+\frac{r_{k,i}}{2\lambda_{k,i}}\theta_{k,i}^{2}. \tag{49}$$

Then, we define $W_k = W_{k,n}+\bar{W}_k$ and have

$$\begin{aligned} LW_k \leq & -\sum_{i=1}^{n}\frac{\kappa}{\kappa+3}s_{k,i}v_{k,i}^{\kappa+3}-\sum_{i=1}^{n}\frac{3}{\kappa+3}s_{k,i}\vartheta_{k,i}^{\kappa+3} \\ & -\sum_{i=1}^{n}\frac{r_{k,i}}{2\lambda_{k,i}}\tilde{\theta}_{k,i}^{2}+\sum_{i=1}^{n}\frac{r_{k,i}}{2\lambda_{k,i}}\theta_{k,i}^{2}+\sum_{i=1}^{n}\Gamma_{k,i} \\ & +\bar{\Gamma}_k-\left(\frac{3}{4}t_{k,1}-\frac{3}{2}\left(o_k+\sum_{j=1}^{N}\rho_{k,j}\right)\right)\vartheta_{k,1}^{4} \\ & -\left(\frac{3}{4}t_{k,2}-\frac{3}{2}-\frac{1}{4}\left(o_k+\sum_{j=1}^{N}\rho_{k,j}\right)\right)\vartheta_{k,2}^{4} \\ & -\left(\frac{3}{4}t_{k,3}-\frac{7}{4}\right)\vartheta_{k,3}^{4}-\cdots-\left(\frac{3}{4}t_{k,n}-\frac{1}{4}\right)\vartheta_{k,n}^{4}, \end{aligned} \tag{50}$$

Based on Lemma 4, choosing $x = \sum_{i=1}^{n}\frac{r_{k,i}}{2\lambda_{k,i}}\tilde{\theta}_{k,i}^{2}$, $z = 1$, $p = \frac{\kappa+3}{4}$, $q = 1-p = \frac{1-\kappa}{4}$, $\alpha(x,z) = \frac{4}{\kappa+3}$, we obtain

$$\begin{aligned} \left(\sum_{j=1}^{n}\frac{r_{k,i}}{2\lambda_{k,i}}\tilde{\theta}_{k,i}^{2}\right)^{\frac{\kappa+3}{4}} \leq & \sum_{i=1}^{n}\frac{r_{k,i}}{2\lambda_{k,i}}\tilde{\theta}_{k,i}^{2} \\ & +\frac{1-\kappa}{4}\left(\frac{4}{\kappa+3}\right)^{-\frac{\kappa+3}{1-\kappa}} \end{aligned} \tag{51}$$

Let $\frac{3}{4}t_{k,1}-\frac{3}{2}(o_k+\sum_{j=1}^{N}\rho_{k,j}) = 0$, we can obtain $t_{k,1} = 2(o_k+\sum_{j=1}^{N}\rho_{k,j})$; similarly, $t_{k,2} = 2+\frac{1}{3}(o_k+\sum_{j=1}^{N}\rho_{k,j}), t_{k,3} = \cdots t_{k,n-1} = \frac{7}{3}, t_{k,n} = \frac{1}{3}$. Substituting that into (50) yields

$$\begin{aligned} LW_k \leq & -\sum_{i=1}^{n}\frac{\kappa}{\kappa+3}s_{k,i}v_{k,i}^{\kappa+3}-\sum_{i=1}^{n}\frac{3}{\kappa+3}s_{k,i}\vartheta_{k,i}^{\kappa+3} \\ & -\left(\sum_{i=1}^{n}r_{k,i}\frac{1}{2\lambda_{k,i}}\tilde{\theta}_{k,i}^{2}\right)^{\frac{\kappa+3}{4}}+\Gamma_k, \end{aligned} \tag{52}$$

where $\Gamma_k = \sum_{i=1}^{n}\frac{r_{k,i}}{2\lambda_{k,i}}\theta_{k,i}^{2}+\sum_{i=1}^{n}\Gamma_{k,i}+\bar{\Gamma}_k+\frac{1-\kappa}{4}(\frac{4}{\kappa+3})^{-\frac{\kappa+3}{1-\kappa}}$.

Let $\Delta_k = \min\{4^{\frac{\kappa+3}{4}}\frac{\kappa}{\kappa+3}s_{k,i}, 4^{\frac{\kappa+3}{4}}\frac{3}{\kappa+3}s_{k,i}, r_{k,i}\}$, then we have

$$LW_k \leq -\Delta_k W_k^{\frac{\kappa+3}{4}} + \Gamma_k, \tag{53}$$

Further consider a Lyapunov function as

$$W = \sum_{k=1}^{N} W_k, \tag{54}$$

we have

$$LW = -\sum_{k=1}^{N} \Delta_k W_k^{\frac{\kappa+3}{4}} + \sum_{k=1}^{N} \Gamma_k. \tag{55}$$

Let $\Delta = \min\{\Delta_k\}$, $\Gamma = \sum_{k=1}^{N} \Gamma_k$, we obtain

$$LW \leq -\Delta \sum_{k=1}^{N} W_k^{\frac{\kappa+3}{4}} + \Gamma, \tag{56}$$

Based on Lemma 3, we have

$$LW \leq -\Delta(\sum_{k=1}^{N} W_k)^{\frac{\kappa+3}{4}} + \Gamma = -\Delta W^{\frac{\kappa+3}{4}} + \Gamma. \tag{57}$$

Consider $W(z(t)) = W$, for $0 \leq s \leq t$, using the Itô formula, we get

$$\begin{aligned} E[W(z(t))] &= EW(z(s)) + E\int_s^t LW(z(v))\mathrm{dv} \\ &= EW(z(s)) + \int_s^t E[LW(z(v))]\mathrm{dv}. \end{aligned} \tag{58}$$

According to (53), with Jensen's inequality, the (58) can be rewritten as

$$\begin{aligned} E[LW(z(v))] &\leq -\Delta E[W^{\frac{\kappa+3}{4}}(z(v))] + \Gamma \\ &\leq -\Delta[E[W(z(v))]]^{\frac{\kappa+3}{4}} + \Gamma. \end{aligned} \tag{59}$$

Substituting (59) into (58) yields

$$\begin{aligned} E[W(z(t))] \leq\, & E[W(z(s))] \\ & + \int_s^t \{-\Delta[E[W(z(v))]]^{\frac{\kappa+3}{4}} + \Gamma\}\mathrm{dv}, \end{aligned} \tag{60}$$

Therefore,

$$\begin{aligned} & E[W(z(t))] - E[W(z(s))] \\ & \leq -\Delta\int_s^t [E[W(z(v))]]^{\frac{\kappa+3}{4}}\mathrm{dv} + \Gamma(\mathrm{t}-\mathrm{s}). \end{aligned} \tag{61}$$

According to Lemma 5, by applying $W(\zeta(t)) = E[W(z(t))]$, we can infer that there exists a setting time $\bar{T} = \frac{4}{(1-\kappa)\sigma\Delta}[E[W(z(t))]]^{\frac{1-\kappa}{4}} - (\frac{\Gamma}{(1-\sigma)\Delta})^{\frac{1-\kappa}{\kappa+3}}] + T$, such that $E[W(z(t))] \leq \epsilon$ for $\forall t \geq \bar{T}$, where $\epsilon = 4(\frac{\Gamma}{(1-\sigma)\Delta})^{\frac{1}{\kappa+3}}$.

According to the definition of $W(z(t))$, the following inequality is satisfied:

$$E\left(\sum_{k=1}^{N}\sum_{i=1}^{n} v_{k,i}^4\right) \leq 4E[W(z(t))] \leq 4\epsilon, t \geq \bar{T}. \tag{62}$$

By the property of mathematical expectation, we obtain

$$\begin{aligned} & \left[E|v_{k,i}|^2\right]^2 \leq E\left(v_{k,i}^4\right) \\ & \leq E\left(\sum_{k=1}^{N}\sum_{j=1}^{n} v_j^4\right) \leq 4\epsilon, t \geq \bar{T}. \end{aligned} \tag{63}$$

Thus

$$E|v_{k,i}|^2 \leq 2\sqrt{\epsilon}, t \geq \bar{T}. \tag{64}$$

Similarly, we get

$$E|\vartheta_{k,i}|^2 \leq 2\sqrt{\epsilon}, E|\tilde{\theta}_{k,i}|^2 \leq 2\sqrt{\epsilon}, t \geq \bar{T}. \tag{65}$$

Since $v_{k,1} = \mu_{k,1} - \vartheta_{k,1}$, one has

$$E|\mu_{k,1}|^2 \leq 2E|v_{k,i}|^2 + 2E|\vartheta_{k,i}|^2 \leq 4\sqrt{\epsilon}, t \geq \bar{T}. \tag{66}$$

Denote $\mu = [\mu_{1,1}, \mu_{2,1}, \ldots, \mu_{k,1}]^T$ and $\Xi = [y_1 - y_d, y_2 - y_d, \ldots, y_k - y_d]^T$, from (7) and Assumption 1, we can obtain $\Xi = (H \otimes I_{k\times k})^{-1}\mu$. Then denoting $\sigma_{\min}(H)$ as the minimum singular value of H, we have $E|y_i - y_d|^2 \leq [\sqrt{N}E|\mu|^2/\sigma_{\min}(H)] \leq [4\sqrt{N}\sqrt{\epsilon}/\sigma_{\min}(H)]$, in finite-time $t \geq T$. The proof is now complete. □

Remark 6 The mean square of tracking error $E|\mu_{k,1}|^2$ is less than $4\sqrt{\epsilon}$ when $t > \bar{T}$, where $\epsilon = 4(\frac{\Gamma}{(1-\tau)\Delta})^{\frac{1}{\kappa+3}}$. As a result, we can choose small $l_{k,i}$, $b_{k,i}$ and $r_{k,i}$ to ensure a smaller Γ, while large parameters $s_{k,i}$ and $r_{k,i}$ can ensure a larger Δ. The smaller Γ and larger Δ can ensure the lower mean square of tracking error $E|\mu_{k,1}|^2$, and the closed-loop system has a faster convergence time from the definition of $\bar{T}$. Note that although the approximation error $\varepsilon_{k,i}$ is unknown, it can be adjusted by choosing proper node number of FLS. The parameter M is the number of the fuzzy rules, if M is too small, the approximation may be under-fitting, while too large M may not reduce the approximation error but increase the computation burden. So the parameter M should be chosen properly by trial and error. At last, [47] gives how to choose the filter gains for (8), that is $\varsigma_{k,i,2}$ should be chosen first and $\varsigma_{k,i,1}$ and $\varsigma_{k,i,2}$ should be sufficiently large.

Remark 7 As shown in Fig. 1, a composite control structure based on FTCF (8), auxiliary system (13), error compensation system (15), and adaptive law (12) is proposed to achieve the desired control performance. Although the FTCF and error compensation system

increase the complexity of the control structure, but can eliminate the complex calculation for the derivative of virtual control functions, so the computational complexity is actually reduced compared with the traditional back-stepping-based algorithms in [41–43]. Further, we use the estimating of parameter $\theta_{k,i}$ instead of estimating the weight vector $V_{k,i}$ to further simply adaptive updating laws design. Although the conservatism of the estimation is increased, it also reduces the complexity of the algorithm to a certain extent.

Remark 8 Since the FLS is used to approximate the unknown nonlinear dynamics, and Assumption 3 is needed to guarantee the application of FLS, only the semi-global results can be secured, which will bring the limit of the proposed algorithm. Further study will focus on how to design the approximation-free algorithm such that the global results can be obtained.

4 Simulation Results

Example 1 Firstly, we will use a numerical example to test the suggested approach. Figure 2 shows the communication topology of a second-order stochastic multi-agent system with one leader and three followers under a directed graph. The Laplacian matrix is described as $\begin{bmatrix} 0 & 0 & 0 \\ -1 & 1 & 0 \\ -1 & 0 & 1 \end{bmatrix}$ and the leader adjacency matrix is described as $\begin{bmatrix} 1 & 0 & 0 \\ 0 & 0 & 0 \\ 0 & 0 & 0 \end{bmatrix}$. The system functions are described as

$$
\begin{aligned}
&y_d = sin(t),\\
&f_{1,1} = x_{1,1}\sin(x_{1,1}), g_{1,1} = 0.25x_{1,1}\sin(x_{1,1}),\\
&f_{1,2} = x_{1,1}x_{1,2}, g_{1,2} = 0.5x_{1,1}e^{x_{1,2}},\\
&f_{2,1} = x_{2,1}\sin(0.5x_{2,1}), g_{2,1} = 0.25x_{2,1},\\
&f_{2,2} = x_{2,1}x_{2,2}, g_{2,2} = 0.5e^{x_{2,2}},\\
&f_{3,1} = x_{3,1}\cos(x_{3,1}), g_{3,1} = -\cos(0.5x_{3,1}),\\
&f_{3,2} = x_{3,1}x_{3,2}, g_{3,2} = x_{3,1}e^{-0.5x_{3,2}},\\
&x_1(0) = [-0.1, 0.25], \mathrm{x}_2(0) = [0.1, 0.3],\\
&x_3(0) = [0.15, -0.2].
\end{aligned}
\tag{67}
$$

The input saturation for $u_k(k = 1, 2, 3)$ is considered as $u_k = \mathrm{sat}(\tau_k) = \begin{cases} 15, \tau_k \geq 15 \\ \tau_k, -15 < \tau_k < 15 \\ -15, \tau_k \leq -15 \end{cases}$. The control parameters are chosen as $t_{k,1} = 2, t_{k,2} = 1/3$, $s_{k,1} = 10, s_{k,2} = 60$, $\lambda_{k,1} = 20, \lambda_{k,2} = 5$, $r_{k,1} = r_{k,2} = 100$, $b_{k,1} = b_{k,2} = 1, k = 1, 2, 3$, and $\kappa = 3/5$. The number of fuzzy ruler for FLS is 10, the centers of basis function are distributed evenly in $[-2, 2] \times \cdots \times [-2, 2]$, and the width is chosen as 4.

Figures 3, 4, 5, and 6 give the response curves of Example 1 under the scheme FTCFB. Figure 3 shows the trajectories of followers $y_k, (k = 1, 2, 3)$ and the leader y_d under the proposed control scheme. Figure 4 shows that the input saturation is not violated by the response curves of u_k. It shows the trajectories of $\chi_{k,1}$ and $\varphi_{k,2}$ based on FTCF in Fig. 5. Clearly, the intermediate signals may be quickly filtered out by the filter. Figure 6 shows the curves of estimated value $\hat{\theta}_{k,i}$.

When taking $\kappa = 1$, the control algorithm degenerates to the asymptotically convergent algorithm in [35]. To compare with the control effect of the proposed algorithm in

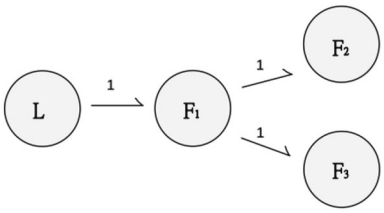

Fig. 2 Communication topology

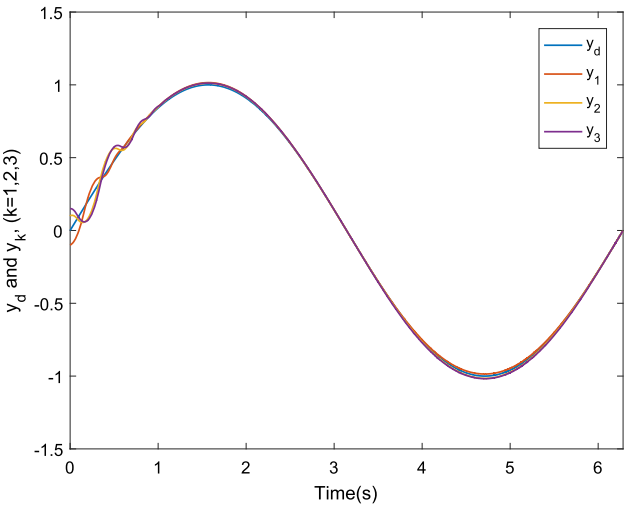

Fig. 3 Trajectories curves of y_d and y_k, $k = 1, 2, 3$

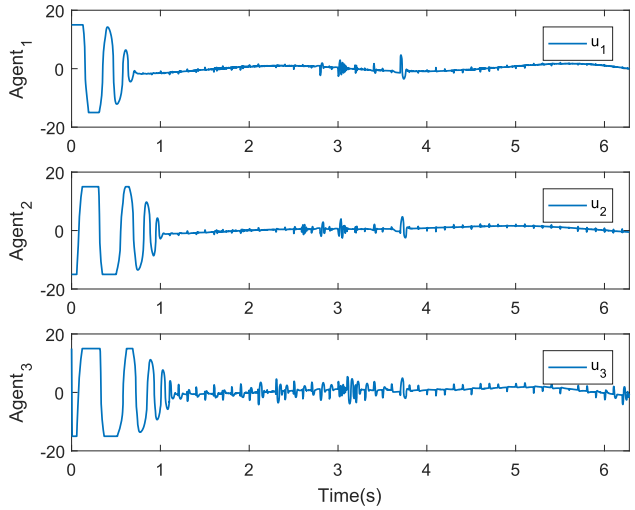

Fig. 4 Trajectories curves of $u_k, k = 1, 2, 3$

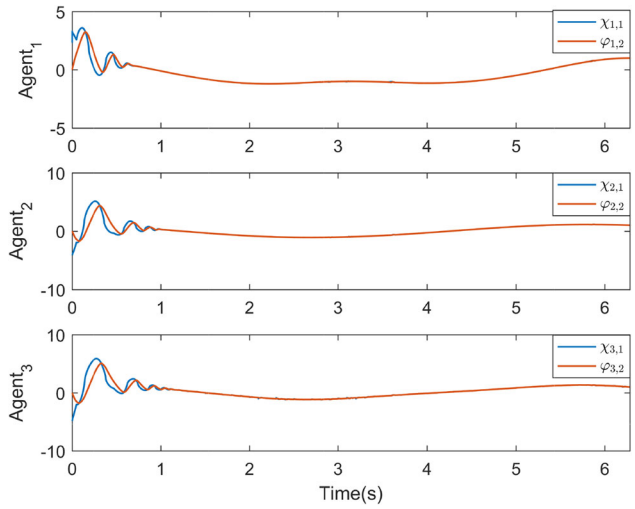

Fig. 5 Trajectories curves of $\varphi_{k,2}$ and $\chi_{k,1}, k = 1, 2, 3$

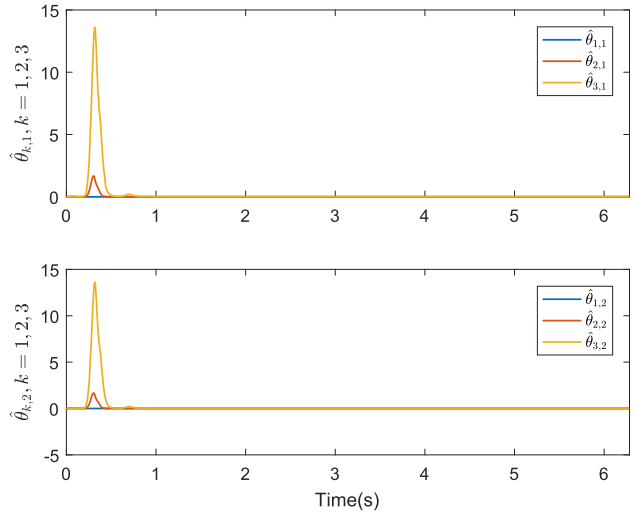

Fig. 6 Trajectories curves of $\hat{\theta}_{k,i}, k = 1, 2, 3, i = 1, 2$

[35], we define an overall tracking error $\mathrm{OTE} = \sqrt{\sum_{k=1}^{3} \|z_{k,1} - y_d\|^2}$ and a root-mean-square error $\mathrm{RMSE} = \sqrt{\frac{\sum_{k=1}^{3}\sum_{i=1}^{K}(z_{k,1}(i)-y_d(i))^2)}{K}}$, where K is the total number of samples and i is the sample index.

Figure 7 shows the state trajectories of $\kappa = 1$. The OTE with different κ is shown in Fig. 8 and the comparison results of RMSE are given in Table 1. It can be seen that the although the convergence rate is faster when $\kappa = 1$ in [35], but the steady-state performance is inferior to our algorithm.

Example 2 Secondly, we further consider the multiple single-link manipulators system to show the effectiveness of the proposed algorithm, and the same communication topology as in Example 1 is chose. For each manipulator, the dynamics is

$$M_k(q_k)\ddot{q}_k + C_k(q_k, \dot{q}_k)\dot{q}_k = u_k + \Lambda_k(q_k)\xi_k, \tag{68}$$

where $k = 1, 2, 3$, q_k denotes the arm's position, $\dot{q}_k$ is the angular velocity, u_k is the control input subjected to input constraint, respectively. For each follower, $M_k(q_k) \in \mathbf{R}$ is the inertia matrix , $C_k(q_k, \dot{q}_k) \in \mathbf{R}$ is the centripetal matrix, $\Lambda_k(q_k) \in \mathbf{R}$ and $\Lambda_k(q_k)\xi_k$ is the random excitation force caused by the white noise ξ_k, which are defined as

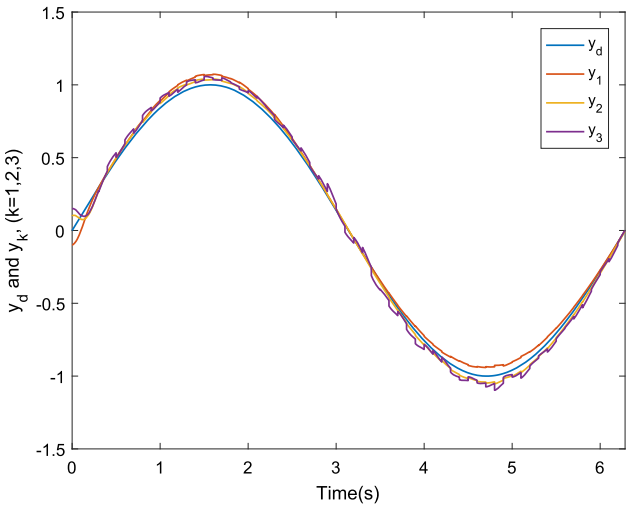

Fig. 7 Trajectories curves y_d and y_k, $k = 1, 2, 3$ in [35]

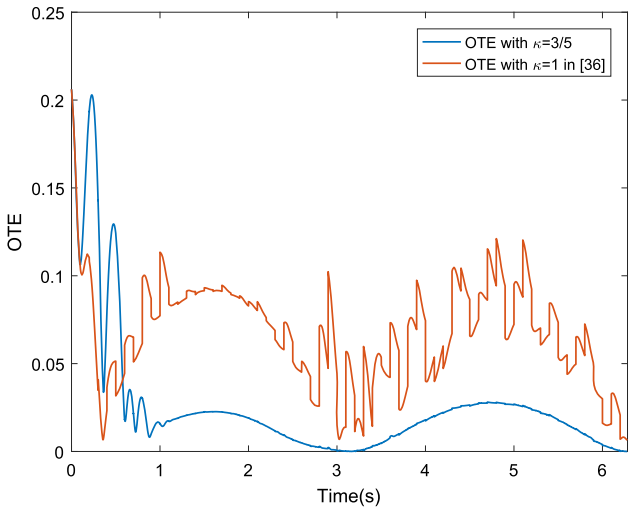

Fig. 8 OTE with $\kappa = 1$ in [35] and $\kappa = 3/5$

Table 1 Performance comparisons of Example 1

Algorithm	RMSE(rad)
FTCFB	0.0256
CFB in [35]	0.0695

$$
\begin{aligned}
&y_d = \cos(0.75t) + \sin(2t),\\
&M_1(q_1) = m_1 {L_1}^2, C_1(q_1, \dot{q}_1) = m_1 g L_1 \sin(q_1),\\
&\Lambda_1(q_1) = -m_1 L_1 \cos(q_1),\\
&M_2(q_2) = m_2 {L_2}^2, C_2(q_2, \dot{q}_2) = m_2 g L_2 \sin(0.5 q_2),\\
&\Lambda_2(q_2) = -m_2 L_2 \cos(q_2),\\
&M_3(q_3) = m_3 {L_3}^2, C_3(q_3, \dot{q}_3) = m_3 g L_3 \sin(0.5 q_3),\\
&\Lambda_3(q_3) = -m_3 L_3 \cos(q_3),\\
&[q_1(0), \dot{q}_1(0)] = [-0.1, -0.25],\\
&[q_2(0), \dot{q}_2(0)] = [-0.1, 0.3],\\
&[q_3(0), \dot{q}_3(0)] = [-0.1, -0.3].
\end{aligned}
\tag{69}
$$

The parameters of them are chosen as in Table 2. The input saturation for $u_k (k = 1, 2, 3)$ is considered as $u_k = \mathrm{sat}(\tau_k) = \begin{cases} 50, \tau_k \geq 50 \\ \tau_k, -50 < \tau_k < 50. \\ -50, \tau_k \leq -50 \end{cases}$ The parameters of the control signals are selected as $t_{k,1} = 2, t_{k,2} = 1/3$, $s_{k,l} = 15, s_{k,2} = 90$, $\lambda_{k,l} = 200, \lambda_{k,2} = 250$, $r_{k,l} = r_{k,2} = 100$, $b_{k,1} = b_{k,2} = 1, k = 1, 2, 3$, and $\kappa = 3/5$. Similarly to Example 1, the number of fuzzy ruler for FLS is 10, the centers of basis function are distributed evenly in $[-2, 2] \times \cdots \times [-2, 2]$, and the width is chosen as 4.

Table 2 Parameters in a single-link manipulator systems

Description	Values	Unit
The mass of the link	$[m_1, m_2, m_3] = [0.5, 0.6, 0.5]$	kg
The distance of the link	$[l_1, l_2, l_3] = [0.25, 0.3, 0.25]$	m
Acceleration of gravity	$g = 9.8$	m/s^2

Figures 9, 10, 11, and 12 give the response curves of Example 2 under the scheme FTCFB, Fig. 9 shows the state $q_k, (k = 1, 2, 3)$ and leader's output y_d, it can also be seen that q_k tracks the desired output y_d commendably. Figures 10 and 11 give the response curves of controller and command filter; it shows that the input saturation is not violated and the intermediate signals may be quickly filtered by the filter. Fig. 12 gives response curves of adaptive law $\hat{\theta}_k, (k = 1, 2, 3)$. Figures 13 and 14 give the response curves of Example 2 under the scheme CFB in [35], Fig. 13 shows the response curves of leader and followers, and Fig. 14 gives the response curves of OTE under FTCFB and CFB, respectively. The RMSE under different algorithms is given in Table 3. Similarly to Example 1, it can be seen the proposed FTCFB can obtain the better steady-state performance than CFB in [35].

Remark 9 Note that the basic principle for choosing the control parameters and filter parameters have been introduced in Remark 6. Actually, in simulations and applications, we should first follow the basic principle in Remark 6, then we can test several sets of the control parameters satisfying Remark 6 by trail and error to achieve a better control effect.

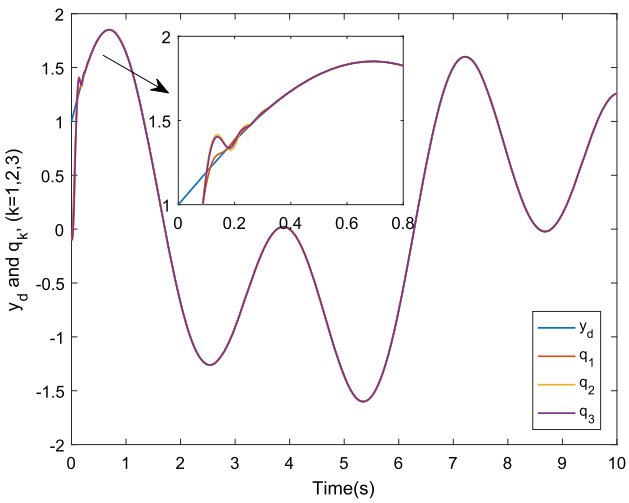

Fig. 9 Trajectories curves of y_d and q_k, $k = 1, 2, 3$

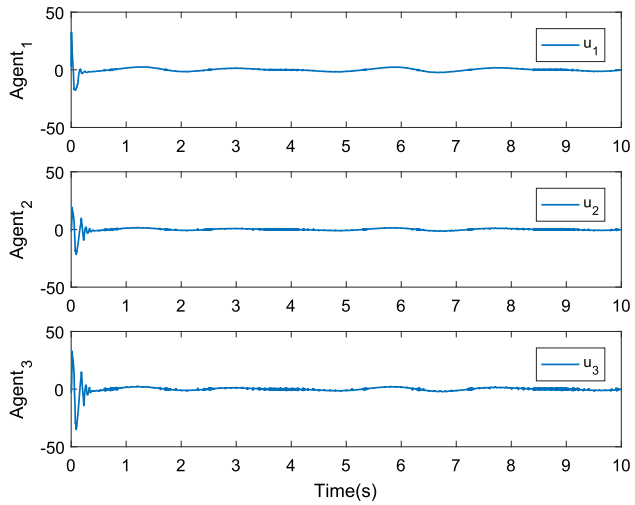

Fig. 10 Trajectories curves of u_k, $k = 1, 2, 3$

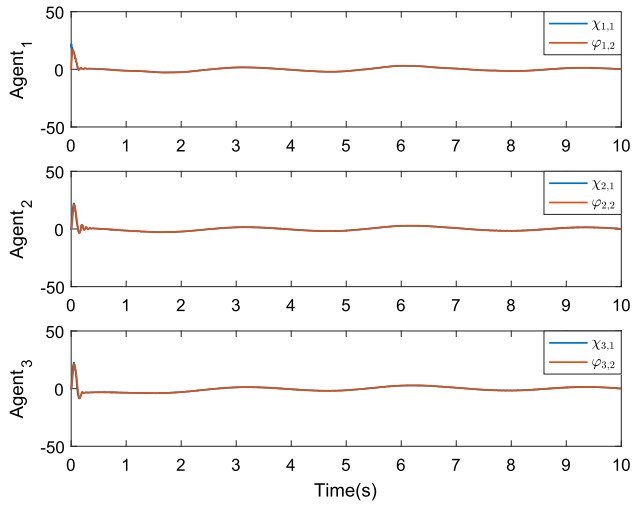

Fig. 11 Trajectories curves of $\varphi_{k,2}$ and $\chi_{k,1}$, $k = 1, 2, 3$

5 Conclusion

A new control method based on FTCFB and FLS is presented in this paper to achieve consensus tracking of high-order SNMASs under input saturation. At the controller design stage, the FLS is utilized to approximate unknown nonlinear dynamics. The FTCFB not only guarantees the tracking error of high-order SNMASs that is practically finite-time stable in mean square, but also avoids the problem of high-gain and the singularity problem. Furthermore, the implementation of the command filter

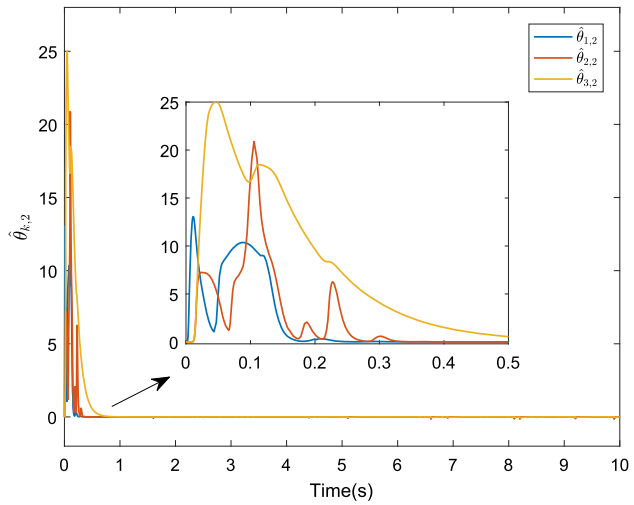

Fig. 12 Trajectories curves of $\hat{\theta}_{k,2}, k = 1, 2, 3$

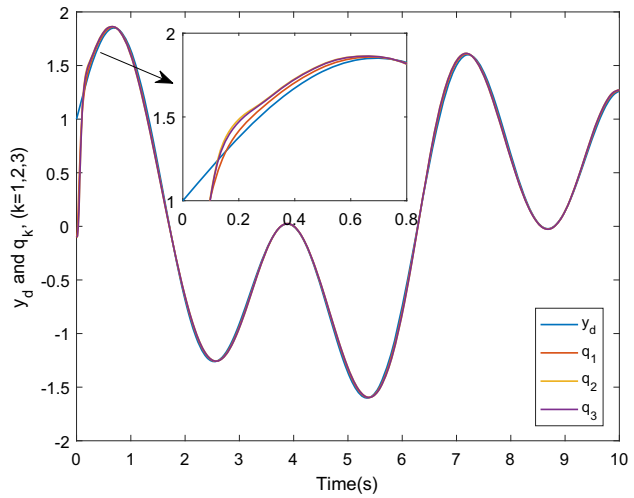

Fig. 13 Trajectories curves y_d and q_k, $k = 1, 2, 3$ in [35]

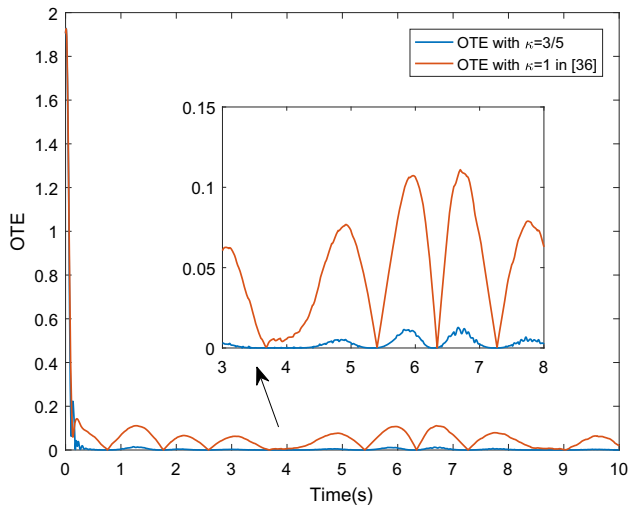

Fig. 14 OTE with $\kappa = 1$ in [35] and $\kappa = 3/5$

Table 3 Performance Comparisons of Example 2

Algorithm	RMSE(rad)
FTCFB	0.0904
CFB in [35]	0.3063

eliminates the POCE of traditional backstepping. The numerical example verified the proposed theoretical results. The future research direction will be the output feedback case with extended state observer.

Acknowledgements This work was supported by the National Natural Science Foundation of China (61603204), the Natural Science Foundation of Shandong Province (ZR2021MF046), the Science and Technology Support Plan for Youth Innovation of Universities in Shandong Province (2019KJN033), and the Taishan Scholar Special Project Fund (TS20190930).

References

1. Fax, J.A., Murray, R.M.: Information flow and cooperative control of vehicle formations. IEEE Trans. Autom. Control **49**(9), 1465–1476 (2004)
2. Nuno, E., Ortega, R., Basanez, L., Hill, D.: Synchronization of networks of nonidentical Euler-lagrange systems with uncertain parameters and communication delays. IEEE Trans. Autom. Control **56**(4), 935–941 (2011)
3. Tang, Y., Xing, X., Karimi, H.R., Kocarev, L., Kurths, J.: Tracking control of networked multi-agent systems under new characterizations of impulses and its applications in robotic systems. IEEE Trans. Ind. Electron. **63**(2), 1299–1307 (2016)
4. Zheng, M., Liu, C., Liu, F.: Average-consensus tracking of sensor network via distributed coordination control of heterogeneous multi-agent systems. IEEE Control Syst. Lett. **3**(1), 132–137 (2019)
5. Cui, M., Wu, Z., Xie, X.: Output feedback tracking control of stochastic Lagrangian systems and its application. Automatica **50**(5), 1424–1433 (2014)
6. Cui, M., Wu, Z., Xie, X., Shi, P.: Modeling and adaptive tracking for a class of stochastic Lagrangian control systems. Automatica **49**(3), 770–779 (2013)
7. Zhao, L., Jia, Y.: Finite-time attitude stabilisation for a class of stochastic spacecraft systems. IET Control Theory. Appl. **9**(8), 1320–1327 (2015)
8. Xu, Y.J., Xin, M.: Nonlinear stochastic control for space launch vehicles. IEEE Trans. Aerosp. Electron. Syst. **47**(1), 98–108 (2011)
9. Cheng, W., Xue, H., Liang, H., Wang, W.: Prescribed performance adaptive fuzzy control of stochastic nonlinear multi-agent systems with input hysteresis and saturation. Int. J. Fuzzy Syst. (2021). https://doi.org/10.1007/s40815-021-01112-y
10. Yoo, S.J.: Distributed adaptive containment control of uncertain nonlinear multi-agent systems in strict-feedback form. Automatica **49**(7), 2145–2153 (2013)
11. You, X., Hua, C.-C., Yu, H.-N., Guan, X.-P.: Leader-following consensus for high-order stochastic multi-agent systems via dynamic output feedback control. Automatica **107**, 418–424 (2019)
12. Shen, H., Li, F., Cao, J., Wu, Z., Lu, G.: Fuzzy-model-based output feedback reliable control for network-based semi-Markov jump nonlinear systems subject to redundant channels. IEEE Trans. Cybern. **50**(11), 4599–4609 (2020)
13. Shen, H., Xing, M., Wu, Z., Xu, S., Cao, J.: Multiobjective fault-tolerant control for fuzzy switched systems with persistent dwell time and its application in electric circuits. IEEE Trans. Fuzzy Syst. **28**(10), 2335–2347 (2020)
14. Zou, L., Wang, Z., Gao, H., Alsaadi, F.E.: Finite-horizon H_∞ consensus control of time-varying multiagent systems with stochastic communication protocol. IEEE Trans. Cybern. **47**(8), 1830–1840 (2017)
15. Ma, L., Wang, Z., Lam, H.-K.: Mean-square H_∞ consensus control for a class of nonlinear time-varying stochastic multiagent systems: the finite-horizon case. IEEE Trans. Syst. Man Cybern. Syst. **47**(7), 1050–1060 (2017)
16. Nandanwar, A., Dhar, N.K., Malyshev, D., Rybak, L., Behera, L.: Stochastic event-based super-twisting formation control for multi-agent system under network uncertainties. IEEE Trans. Control Netw. Syst. (2021). https://doi.org/10.1109/TCNS.2021.3089142
17. Wang, W., Wen, C., Huang, J.: Distributed adaptive asymptotically consensus tracking control of nonlinear multi-agent systems with unknown parameters and uncertain disturbances. Automatica **77**, 133–142 (2017)
18. Zhao, D., Zou, T., Li, S., Zhu, Q.: Adaptive backstepping sliding mode control for leader-follower multi-agent systems. IET Control Theory Appl. **6**(8), 1109–1117 (2012)
19. Zhao, L., Yu, J., Yu, H., Lin, C.: Neuroadaptive containment control of nonlinear multiagent systems with input saturations. Int. J. Robust Nonlinear Control **29**(9), 2742–2756 (2019)
20. Wang, Y., Song, Y.: Fraction dynamic-surface-based neuroadaptive finite-time containment control of multiagent systems in nonaffine pure-feedback form. IEEE Trans. Neural Netw. Learn. Syst. **28**(3), 678–689 (2017)
21. Farrell, J.A., Polycarpou, M., Sharma, M., Dong, W.: Command filtered backstepping. IEEE Trans. Autom. Control **54**(6), 1391–1395 (2009)
22. Dong, W., Farrell, J.A., Polycarpou, M.M., Djapic, V., Sharma, M.: Command filtered adaptive backstepping. IEEE Trans. Control Syst. Technol. **20**(3), 566–580 (2012)
23. Cui, G., Xu, S., L. Lewis, F., Zhang, B., Ma, Q.: Distributed consensus tracking for non-linear multi-agent systems with input saturation: a command filtered backstepping approach. IET Control. Theory Appl. 10(5), 509–516 (2016)
24. Shen, Q., Shi, P.: Distributed command filtered backstepping consensus tracking control of nonlinear multiple-agent systems in strict-feedback form. Automatica **53**, 120–124 (2015)
25. Zhao, L., Yu, J., Lin, C.: Command filter based adaptive fuzzy bipartite output consensus tracking of nonlinear coopetition multi-agent systems with input saturation. ISA Trans. **80**, 187–194 (2018)
26. Zhao, L., Yu, J., Lin, C.: Distributed adaptive output consensus tracking of nonlinear multi-agent systems via state observer and command filtered backstepping. Inf. Sci. **478**, 355–374 (2019)
27. Zhao, L., Yu, J.P., Lin, C., Ma, Y.M.: Adaptive neural consensus tracking for nonlinear multiagent systems using finite-time command filtered backstepping. IEEE Trans. Syst. Man Cybern. Syst. **48**(11), 2003–2012 (2018)
28. Deng, H., Krstic, M.: Output-feedback stochastic nonlinear stabilization. IEEE Trans. Autom. Control **44**(2), 328–333 (1999)
29. Duan, N., Xie, X.: Further results on output-feedback stabilization for a class of stochastic nonlinear systems. IEEE Trans. Autom. Control **56**(5), 1208–1213 (2011)
30. Min, H., Xu, S., Zhang, B., Ma, Q.: Output-feedback control for stochastic nonlinear systems subject to input saturation and time-varying delay. IEEE Trans. Autom. Control **64**(1), 359–364 (2019)
31. Homayoun, B., Arefi, M.M., Vafamand, N., Yin, S.: Neuro-adaptive command filter control of stochastic time-delayed

nonstrict-feedback systems with unknown input saturation. J. Franklin Inst. **357**(12), 7456–7482 (2020)
32. Sun, W., Su, S.F., Xia, J., Zhuang, G.: Command filter-based adaptive prescribed performance tracking control for stochastic uncertain nonlinear systems. IEEE Trans. Syst. Man Cybern. Syst. (2020). https://doi.org/10.1109/TSMC.2019.2963220
33. Wang, X., Wu, Q., Yin, X.: Command filter based adaptive control of asymmetric output-constrained switched stochastic nonlinear systems. ISA Trans. **91**, 114–124 (2019)
34. Zhao, Z., Yu, J., Zhao, L., Yu, H., Lin, C.: Adaptive fuzzy control for induction motors stochastic nonlinear systems with input saturation based on command filtering. Inf. Sci. **463–464**, 186–195 (2018)
35. Shahvali, M., Askari, J.: Distributed containment output-feedback control for a general class of stochastic nonlinear multi-agent systems. Neurocomputing **179**, 202–210 (2016)
36. Zou, W., Shi, P., Xiang, Z., Shi, Y.: Finite-time consensus of second-order switched nonlinear multi-agent systems. IEEE Trans. Neural Netw. Learn. Syst. **31**(5), 1757–1762 (2020)
37. Zou, W., Ahn, C.K., Xiang, Z.: Fuzzy-approximation-based distributed fault-tolerant consensus for heterogeneous switched nonlinear multiagent systems. IEEE Trans. Fuzzy Syst. **29**(10), 2916–2925 (2021)
38. Chen, W., Jiao, L.C.: Finite-time stability theorem of stochastic nonlinear systems. Automatica **46**(12), 2105–2108 (2010)
39. Yin, J., Khoo, S., Man, Z., Yu, X.: Finite-time stability and instability of stochastic nonlinear systems. Automatica **47**(12), 2671–2677 (2011)
40. Khoo, S., Yin, J., Man, Z., Yu, X.: Finite-time stabilization of stochastic nonlinear systems in strict-feedback form. Automatica **49**(5), 1403–1410 (2013)
41. Wang, F., Chen, B., Sun, Y., Gao, Y., Lin, C.: Finite-time fuzzy control of stochastic nonlinear systems. IEEE Trans. Cybern. **55**(6), 2617–2626 (2019)
42. Wang, F., Zhang, Y., Zhang, L., Zhang, J., Huang, Y.: Finite-time consensus of stochastic nonlinear multi-agent systems. Int. J. Fuzzy Syst. **22**(1), 77–88 (2019)
43. Yao, Y., Tan, J., Wu, J.: Event-triggered finite-time adaptive fuzzy tracking control for stochastic nontriangular structure nonlinear systems. Int. J. Fuzzy Syst. (2021). https://doi.org/10.1007/s40815-021-01085-y
44. Fu, Z., Wang, N., Song, S., Wang, T.: Adaptive fuzzy finite-time tracking control of stochastic high-order nonlinear systems with a class of prescribed performance. IEEE Trans. Fuzzy Syst. **30**(1), 88–96 (2022)
45. Wang, N., Tao, F., Fu, Z., Song, S.: Adaptive fuzzy control for a class of stochastic strict feedback high-order nonlinear systems with full-state constraints. IEEE Trans. Syst. Man Cybern. Syst. **52**(1), 205–213 (2022)
46. Xia, J., Li, B., Su, S., Sun, W., Shen, H.: Finite-time command filtered event-triggered adaptive fuzzy tracking control for stochastic nonlinear systems. IEEE Trans. Fuzzy Syst. (2020). https://doi.org/10.1109/tfuzz.2020.2985638
47. Levant, A.: Higher-order sliding modes, differentiation and output-feedback control. Int. J. Control **76**(9–10), 924–941 (2003)

Xinyu Song received the B.S. degree in Automation from the Wuhan University of Science and Technology, Wuhan, China, in 2019. She is currently working toward the M.S. degree with the School of Automation, Qingdao University. Her research interests include finite-time control of stochastic nonlinear systems.

Lin Zhao received the B.S. degree in mathematics and applied mathematics from Qingdao University, Qingdao, China, in 2008, the M.S. degree in operational research and cybernetics from the Ocean University of China, Qingdao, in 2011, and the Ph.D. degree in applied mathematics from Beihang University, Beijing, China, in 2016. He is currently a Distinguished Professor at the School of Automation, Qingdao University. He is a recipient of the Shandong Province Fund for Outstanding Young Scholars. His current research interests include finite-time control, distributed control of multi-agent systems, and spacecraft control systems.